

Experimental evidence of electric inhibition in fast electron penetration and of electric-field-limited fast electron transport in dense matter

F. Pisani,^{1,2} A. Bernardinello,¹ D. Batani,¹ A. Antonicci,¹ E. Martinolli,^{1,2} M. Koenig,² L. Gremillet,² F. Amiranoff,² S. Baton,² J. Davies,³ T. Hall,⁴ D. Scott,⁴ P. Norreys,⁵ A. Djaoui,⁵ C. Rousseaux,⁶ P. Fews,⁷ H. Bandulet,⁸ and H. Pepin⁸

¹*Dipartimento di Fisica “G. Occhialini” and INFN, Università degli Studi di Milano Bicocca, Via Emanueli 15, 20126 Milano, Italy*

²*LULI, UMR No. 7605, CNRS-CEA-X-Paris VI, Ecole Polytechnique, 91128 Palaiseau, France*

³*GOLP, Instituto Superior Tecnico, Lisbon, Portugal*

⁴*University of Essex, Colchester CO4 3SQ, United Kingdom*

⁵*Rutherford Appleton Laboratory, Chilton, Didcot, OX11 0QX, United Kingdom*

⁶*Commissariat à l’Energie Atomique, 91680 Bruyères-le Châtel, France*

⁷*University of Bristol, Bristol BS8 1TL, United Kingdom*

⁸*INRS, Energie et Matériaux, J3X1S2 Varennes, Québec, Canada*

(Received 22 June 2000)

Fast electron generation and propagation were studied in the interaction of a green laser with solids. The experiment, carried out with the LULI TW laser (350 fs, 15 J), used K_α emission from buried fluorescent layers to measure electron transport. Results for conductors (Al) and insulators (plastic) are compared with simulations: in plastic, inhibition in the propagation of fast electrons is observed, due to electric fields which become the dominant factor in electron transport.

PACS number(s): 52.40.Nk, 52.50.Jm, 52.70.La

Fast electron generation in laser interactions is an important subject [1–11], recently rediscovered thanks to developments in short-pulse high-energy lasers, and especially to the “fast ignitor” approach to inertial confinement fusion [12,13]. This is based on decoupling the phases of compression and ignition of the nuclear fuel. In the last phase, a high-intensity short-pulse laser is used to generate relativistic electrons which propagate through the compressed capsule, and lose their energy, heating the DT fuel to ignition. Key aspects to assess the feasibility of fast ignition are the characterization of the electron source (temperature, flux and spread angle of the electron beam), and the study of energy deposition of fast electrons in matter.

Theoretically the last problem has been studied by Deutsch *et al.* [14] using a collisional approach based on the stopping power formulas developed for dense plasmas by Val’chuk *et al.* [15]. Another very important aspect influencing fast electron propagation and energy deposition in both compressed and solid density matter has recently been much discussed in literature [16,17], namely, the so called electric inhibition of propagation.

In other words, the penetration of the fast electrons into the target sets up huge electric fields (due to electrostatic charge separation and induction), which prevent any further propagation, unless neutralized by a return current of the free background electrons. Although electric inhibition of fast electron propagation was observed as early as 1982 [5], in this new high intensity regime it may play a fundamental role, depending on material conductivity, and even be the major limiting factor in electron propagation. Some indirect indication on electric effects at very high laser intensities is given in the experiment by Key *et al.* and Wharton *et al.* [11]. Here the laser was focused onto different materials (Cu, Al, CH) and the observed reduced penetration in plastic was “tentatively” (to use the words of the authors) attributed to

electric fields. The limitation in this experiment is that, by shooting on different materials, the propagation medium and the electron source are simultaneously changed, which makes it difficult to separate propagation effects.

A much clearer and direct experimental evidence of electric inhibition of fast electron propagation is given in the works by Hall *et al.* [18] and Batani *et al.* [19]. Here, penetration of fast electron in cold and in shock compressed plastic targets was compared. The changes in material conductivity and the reduction in thickness due to the shock, combined to render electric effects negligible in the compressed targets.

The experiment presented in this Rapid Communication is performed at much higher laser irradiances, which are more directly relevant for the fast ignition. While electric inhibition is also evidenced in our results, the observed behavior is only ascribed to differences in resistivity. Also, we avoided the problem of Key and Wharton’s papers by using multilayer targets: the first layer, where the LULI TW laser was focused, was always Al and the electron source was therefore unchanged. After this, alternatively conductors and insulators were used to compare fast electron propagation in materials with different electrical properties. We clearly evidenced a different propagation in the two materials with *the same* source. Finally a regime of electric-field-limited fast-electron-transport is evidenced, in agreement with theoretical works which predict electric field effects to become the major limiting factor in fast electron propagation in the limiting case of materials with high resistivity and/or low stopping power.

Also, this experiment was realized at 2ω ($\lambda = 529$ nm) and low pedestal at intensities up to 2×10^{19} W/cm². Thanks to the very low pulse pedestal, no preplasma, or only a very short and tenuous one, is expected, so that we can practically speak about the direct interaction of the (green) laser with a

solid. In these conditions we measured the conversion efficiency and the temperature of the produced fast electrons.

In the experiment, the high flux laser, delivering ≈ 5 J on target, with a pulse duration of 350 fs and a contrast ratio better than 10^8 , is focused at normal incidence on the multilayered target. The fast electrons are produced in the first $1.5 \mu\text{m}$ Al layer, cross a “propagation layer” alternatively made of materials with differing electrical properties (CH or Al), and finally reach two layers of fluorescent materials ($20 \mu\text{m}$ Mo and $20 \mu\text{m}$ Pd) where they induce K_α emission, depending on their number and residual energy. By varying the thickness of the propagation layer from shot to shot, we measured the typical penetration range of the electrons in the given material. K_α photons are detected by a charge-coupled-device (CCD) camera outside the interaction chamber, facing the target rear side, and used in single hit mode to allow spectroscopic analysis. A final $50 \mu\text{m}$ plastic layer on the back of the target prevented any spurious K_α emission due to electrons coming from the interaction zone or those escaping the target and coming back to the rear side. The CCD was absolutely calibrated with a ^{109}Cd source. An x-ray pinhole camera (with a resolution of $7 \mu\text{m}$) imaged the focal spot and CR39 plastic ion track detectors measured the energy of the fast ions produced in the interaction.

We carried out two series of shots in which the laser intensity on target was changed by varying its focusing. In the first, the focal spot diameter was $\approx 30 \mu\text{m}$ and the irradiance $I_L \approx 1-2 \times 10^{18} \text{ W/cm}^2$, while in the second one it was $\leq 10 \mu\text{m}$ and $I_L \approx 1-2 \times 10^{19} \text{ W/cm}^2$ (although in this case, the precision in the measurement was reduced due to the pin hole camera resolution). The plastic layer (polyethylene) had a thickness between 50 and $175 \mu\text{m}$, while Al was 6 to $37 \mu\text{m}$ thick at low intensity; at higher irradiances they were respectively 50 to $400 \mu\text{m}$ and 11.5 to $300 \mu\text{m}$ to match the predicted increased penetration.

The use of two tracer layers is a well established method in K_α diagnostics which allows a more precise determination of the number and energy of fast electrons (e.g., see [20]). The ratio of K_α yield of Pd to Mo, *a priori* independent on the total energy of fast electrons (as long as only collisional effects are considered), is shown versus the propagation layer thickness in Fig. 1; it refers to Al targets at $I_L \approx 1-2 \times 10^{18} \text{ W/cm}^2$. Results were compared with simulations made for different temperatures with the PROPEL Monte Carlo code, which calculates the energy loss and the angular scattering of fast electrons as due to collisions with the target electrons and ions [21]. K_α yield is calculated taking into account the target self-absorption. Electrons are injected perpendicularly into the target. The results, however, are quite insensitive to the initial spread if values $\leq 30^\circ$ are used (as reported in [11,19]), i.e., scattering in the target dominates over the initial spread, which is reasonable for our not-too-energetic electrons, and target thickness (as also deduced by analytical models [22]). Simulations reproduce experimental results, within error bars, with temperatures in the range 175–200 keV. This is consistent with the scaling law by Beg *et al.* [20]. At $I_L \approx 1-2 \times 10^{19} \text{ W/cm}^2$ we found a temperature $\approx 400-500$ keV, again compatible with Beg’s law even if, due to our large experimental error bars, we cannot speak of precise agreement or exclude other scaling laws [23,24].

Figure 2 shows the experimental Mo K_α emission versus

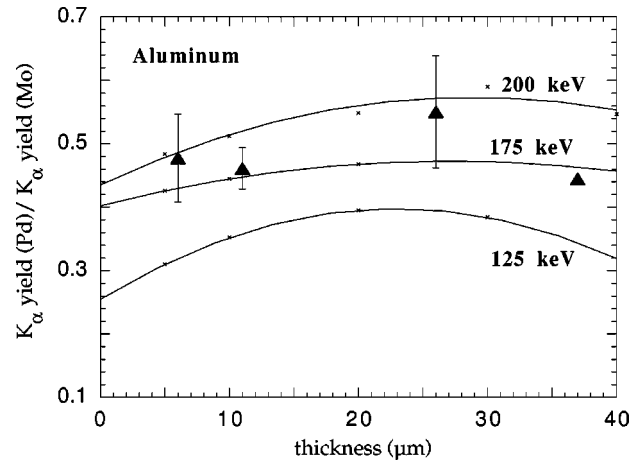


FIG. 1. Experimental (triangles) and numerical (crosses) ratio of Pd and Mo K_α yield (low intensity case). Lines are fits to numerical results, showing a fast electron temperature between 125 and 200 keV.

the propagation layer thickness for both CH and Al targets at $1-2 \times 10^{19} \text{ W/cm}^2$. Exponential fits to the results, i.e., $\exp(-R/R_0)$, give a typical value for the experimental penetration $R_0 \approx 230 \pm 40 \mu\text{m}$ for Al and $180 \pm 30 \mu\text{m}$ for CH. The large error bars are due to fluctuations from shot to shot in laser energy, duration, and focalization, but also, we think, to the very nonlinear aspect of the interaction at such high laser intensities which, for instance, produces random electron jets, as shown in recent works [25–27]. Figure 2 also shows an exponential interpolation of numerical results for a 400 keV temperature. The numerical result for Al ($R_0 = 235 \pm 10 \mu\text{m}$) agrees with the experimental one. The errors on numerical values are obtained by considering the typical shot-to-shot fluctuations in laser pulse and how they influence electron temperature and range. In the case of plastic, there is instead a large discrepancy, the numerical prediction at 400 keV being $690 \pm 20 \mu\text{m}$. Therefore fast electron

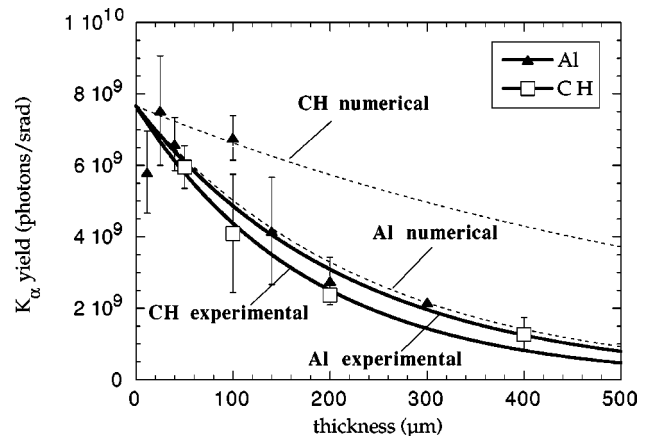


FIG. 2. Experimental and numerical results of Mo K_α yield vs target thickness at $I_L = 1-2 \times 10^{19} \text{ W/cm}^2$. The lines are exponential interpolations of data, indicated by markers, and give for Al a penetration depth of $230 \pm 40 \mu\text{m}$ (experimental) and $235 \pm 10 \mu\text{m}$ (numerical), while for polyethylene the range is $180 \pm 30 \mu\text{m}$ (experimental) and $690 \pm 20 \mu\text{m}$. Error bars on experimental points are the standard deviation of results (no error if there is only a single experimental point at the corresponding thickness).

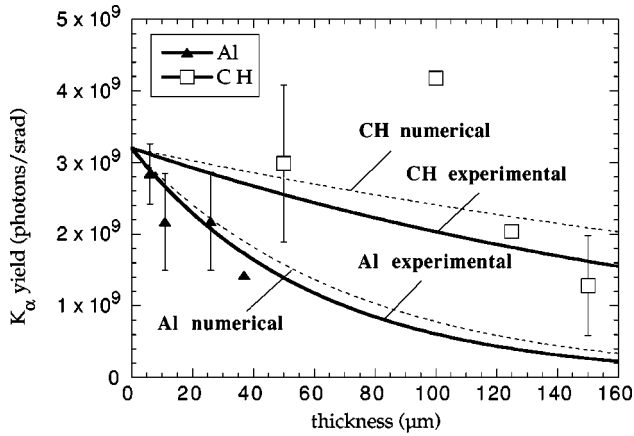


FIG. 3. Experimental and numerical results for Mo K_α yield at $I_L = 1-2 \times 10^{18} \text{ W/cm}^2$. The interpolation give for Al a penetration of $60 \pm 20 \mu\text{m}$ (experimental) and $70 \pm 10 \mu\text{m}$ (numerical), while for polyethylene the range is $220 \pm 50 \mu\text{m}$ (experimental) and $350 \pm 10 \mu\text{m}$. Error bars as in Fig. 2.

propagation in Al is well described by a purely collisional model, while a strong inhibition of penetration is evident in CH.

To understand the results, one must consider the effects of the high electric fields, generated by the fast electrons, which inhibit the propagation unless neutralized by a return current of the background electrons. Therefore, the response of the target strongly depends on material conductivity. Following Bell *et al.* [16], the typical penetration range z_0 due to electric fields alone is

$$z_0 = 3 \times 10^{-3} \sigma_6 T_h^2 (f I_{17})^{-1} \mu\text{m}, \quad (1)$$

where σ_6 is the conductivity in units $10^6 (\Omega\text{m})^{-1}$, T_h is the fast electron temperature in keV, I_{17} is the irradiance on target in units 10^{17} W/cm^2 , and f is the fraction of laser energy converted in fast electrons. Bell's formula can be simply obtained by applying energy conservation and equating the fast electron initial energy ($\approx T_h$) to the work done by the electric field (eEz_0) and by considering that the electric field is proportional to the number of produced fast electrons ($\approx fE_L/T_h$). The main distinction between electric and collisional effects is that the energy loss in the first case is directly proportional to target thickness, while in the latter to areal density ρx . Hence, the use of targets of different densities and electrical properties is a good way to test electric versus collisional effects in fast electron propagation.

Bell's model is a simple analytical 1D model, but it can at least be used to give a qualitative but meaningful explanation of the ongoing physics. A more precise, 2D, modelization of our experiment can be obtained by using the computer code developed by Davies *et al.* [17] and already used in [19] to explain results obtained in [18]. A critical issue for the modelization is the choice of target conductivity. Here we have used a fit to Milchberg's data [17,28,29] for Al, and a simple semiclassical heuristic model for plastic, which is described in detail in [19] (we note, however, that CH electric conductivity at the temperatures we reach in our conditions has never been measured up to now).

Our Al results imply that $z_0 \gg R_{\text{coll}}$, which is indeed found by inserting our experimental parameters in the formula for

z_0 and considering the Al room temperature conductivity [$\sigma_0 = 3.7 \times 10^7 (\Omega\text{m})^{-1}$]. An additional problem is the target heating due to fast electrons. In a very simple way, by considering the volume crossed by fast electrons [22] and an average energy deposition, it is possible to evaluate an Al temperature of a few eV due to such effect. In this temperature range, Al conductivity decreases due to quantum effects although the obtained value is still compatible with our results.

The situation is more complex for CH targets. The conductivity of cold plastic [$\sigma = 10^{-11} (\Omega\text{m})^{-1}$] implies a non-realistically low penetration. Hence, an insulator to conductor phase transition which produces free electrons that are available for the return current is essential to explain fast electron penetration. This is due both to target heating induced by fast electrons and to electric breakdown of plastic (the space charge electric field quickly overcomes that of breakdown by several orders of magnitudes). Although the average temperature reached in plastic is of the same order than in Al, we can infer that electric field effects will remain more important in CH. Also, one must consider that target heating will have opposite effects on Al and CH conductivities, the first being reduced with time as temperature goes up (but keeping quite high values), while the second increases starting practically from zero.

Figure 3 shows the experimental Mo K_α yields versus thickness for low intensity ($1-2 \times 10^{18} \text{ W/cm}^2$). The numerical predictions are $70 \pm 10 \mu\text{m}$ for Al and $350 \pm 10 \mu\text{m}$ for CH for a temperature of 175 keV while the experimental results are $60 \pm 20 \mu\text{m}$ and $220 \pm 50 \mu\text{m}$, respectively. At low intensity, CH results are obtained by fitting a smaller data set which implies larger error bars.

Again, we see that collisional numerical results for Al are in agreement with experiment, within the error bars, while they do not match for CH. With respect to the high intensity case, the experimental penetration in CH is not shorter, but about the same, if not increased. This is a paradox due to the higher electron temperature and can only be explained with electric inhibition, in qualitative agreement with Eq. (1), where the range is inversely proportional to intensity. Also, a collisional explanation must be ruled out in plastic, since it would imply nonrealistically low fast electron temperatures of $\approx 80 \text{ keV}$, in complete disagreement with Al results (the temperature is expected to be the same), and with all published scaling laws [20,23,24]. Furthermore, CR39 data show that the energy of fast ions is the same with CH and Al targets, which again implies the same electron temperature [20].

Simulations performed with the code of Davies *et al.* [17] to take into account electric effects give a penetration range = $200 \mu\text{m}$ in Al and $175 \mu\text{m}$ in CH at high intensity (417 keV). At low intensity (193 keV) we found $63 \mu\text{m}$ for Al and $161 \mu\text{m}$ for CH. The agreement in CH is only qualitative but this is not a serious problem due to the large uncertainty in plastic conductivity.

Finally, it is possible to use K_α yields to obtain the efficiency of energy conversion in fast electrons. The experimental K_α yield must be corrected by considering the CCD collection solid angle, the transmittivity to x-rays of the windows before the CCD and the target self-absorption of K_α photons. Hence, we could match the experimental values to

code predictions (as already done in Figs. 3 and 4) by assuming a conversion factor $f \approx 15 \pm 5\%$ at $I_L = 1 - 2 \times 10^{18} \text{ W/cm}^2$ and $f \approx 25 \pm 5\%$ at $I_L = 1 - 2 \times 10^{19} \text{ W/cm}^2$. We also considered only 50% of the laser energy to be contained in the focal spot (this is a reasonable assumption, also made by other authors [11,20], but not directly measured in our experiment). Thus there is a non-negligible increase in conversion efficiency with intensity. This implies a stronger inhibition at higher intensities in CH; in fact, in Eq. (1) the range is also inversely proportional to the conversion factor (in Al propagation is always dominated by collisions).

In conclusion, the different behavior of plastic and metal targets gives a direct and clear experimental evidence of electric-field inhibition of fast electron propagation in dense matter. In aluminum the large number of background electrons rapidly neutralizes the electric field and inhibition is in first approximation negligible. In plastic the electric response of matter is weaker instead, which leads to inhibition and to

a penetration shorter than predicted by collisional models. From a theoretical basis we do not exclude an influence of electric fields in Al; however, this is far less important and falls within our experimental error bars. Also, we show how in plastic targets the penetration does not increase (actually, within our error bars, it slightly decreases) when the electron energy is increased. This is in complete disagreement with the prediction of collisional models and can only be justified on the basis of electric-field effects, or, in very simple and qualitative terms, by the use of Bell's formula [16]. This gives evidence of a regime of electric-field-limited fast-electron-transport in dense matter.

This work was supported by the TMR European Program, Contract No. ERBFMGECT950044. The participation of A.A. and E.M. was possible within the Erasmus agreement between Università di Milano Bicocca and Ecole Polytechnique.

-
- [1] D. W. Forslund, J. M. Kindel, and K. Lee, *Phys. Rev. Lett.* **39**, 284 (1977).
- [2] J. D. Hares *et al.*, *Phys. Rev. Lett.* **42**, 1216 (1979).
- [3] M. D. Rosen *et al.*, *Phys. Fluids* **22**, 2020 (1979).
- [4] R. J. Harrach and R. E. Kidder, *Phys. Rev. A* **23**, 887 (1981).
- [5] D. J. Bond, J. D. Hares, and J. D. Kilkenny, *Plasma Phys.* **24**, 91 (1982).
- [6] B. Luther Davies, A. Perry, and K. A. Nugent, *Phys. Rev. A* **35**, 4306 (1987).
- [7] G. Malka and J. L. Miquel, *Phys. Rev. Lett.* **77**, 75 (1996).
- [8] F. Amiranoff *et al.*, *J. Phys. A* **43**, 1037 (1982).
- [9] J. D. Lindl, *Phys. Plasmas* **2**, 3933 (1995).
- [10] S. Glenzer *et al.*, *Phys. Rev. Lett.* **81**, 365 (1988).
- [11] M. Key *et al.*, *Phys. Plasmas* **5**, 1966 (1998); K. Wharton *et al.*, *Phys. Rev. Lett.* **81**, 822 (1998).
- [12] M. Tabak *et al.*, *Phys. Plasmas* **1**, 1626 (1994).
- [13] S. Atzeni, *Jpn. J. Appl. Phys., Part 1* **34**, 1980 (1995).
- [14] C. Deutsch *et al.*, *Phys. Rev. Lett.* **77**, 2483 (1996).
- [15] V. V. Val'chuk, N. B. Volkov, and A. P. Yalovets, *Plasma Phys. Rep.* **21**, 159 (1995).
- [16] A. R. Bell *et al.*, *Plasma Phys. Controlled Fusion* **39**, 653 (1997).
- [17] J. Davies *et al.*, *Phys. Rev. E* **56**, 7193 (1997).
- [18] T. A. Hall *et al.*, *Phys. Rev. Lett.* **81**, 1003 (1998); A. Bernardinello *et al.*, *Laser Part. Beams* **17**, 529 (1999).
- [19] D. Batani *et al.*, *Phys. Rev. E* **61**, 5725 (2000).
- [20] F. N. Beg *et al.*, *Phys. Plasmas* **4**, 447 (1997).
- [21] Th. Schlegel *et al.*, *Phys. Rev. E* **60**, 2209 (1999).
- [22] H. H. Hubbel, Jr. and R. D. Birkoff, *Phys. Rev. A* **26**, 2460 (1982).
- [23] M. E. Glinsky, *Phys. Plasma* **2**, 2796 (1995).
- [24] S. Wilks *et al.*, *Phys. Rev. Lett.* **69**, 1383 (1992).
- [25] E. T. Gumbrell *et al.*, *Phys. Plasmas* **5**, 3714 (1998).
- [26] M. Tatarakis *et al.*, *Phys. Rev. Lett.* **81**, 999 (1998).
- [27] L. Gremillet *et al.*, *Phys. Rev. Lett.* **83**, 5015 (1999).
- [28] H. M. Milchberg *et al.*, *Phys. Rev. Lett.* **61**, 2364 (1988).
- [29] Y. T. Lee and R. M. More, *Phys. Fluids* **27**, 1273 (1984).